

Supporting Information

A new anti-biofilm strategy of enabling arbitrary surfaces of materials and devices with robust bacterial anti-adhesion via spraying modified microspheres method

Jietao Hu,^a Jing Lin,^{*a} Yayu Zhang,^a Zekai Lin,^a Zhiwei Qiao,^{*b} Zili Liu,^a Mengyao Dong,^{c,d}
Wei Yang,^a Xiaoguo Liu,^a and Zhanhu Guo^{*c}

a. School of Chemistry and Chemical Engineering, Guangzhou University, Guangzhou 510006, P.R. China.

b. School of Chemistry and Chemical Engineering, South China University of Technology 510641, P.R. China.

c. Integrated Composites Laboratory (ICL), Department of Chemical and Biomolecular Engineering, University of Tennessee, Knoxville, TN 37996, USA.

d. Key Laboratory of Materials Processing and Mold, Zhengzhou University, Zhengzhou 450001, P.R. China.

Experimental Section

Materials. Polyvinylpyrrolidone (PVP, MW=40000 mol g⁻¹), polyethylene glycol maleate (PEGMA), styrene (St), butyl acrylate (BA), 2-hydroxyethyl methacrylate (HEMA), vinyltrimethoxysilane (VTES), glycidyl methacrylate (GMA), iminodiacetic acid (IDA), 2, 2'-azobis (2-methylpropionitrile) (AIBN), and 1H, 1H, 2H, 2H perfluorodecyltrimethoxysilane (PFDTMS) were procured from Sigma Aldrich. Antibacterial monomer was synthesized in our previous work.¹ Silver nitrate (AgNO₃, ≥ 99.8%), hydrochloric acid and aqueous ammonia solution (25 %) were procured from Shanghai Chemical Reagent Co., Ltd. Liquid epoxy resin (Bisphenol A epoxy resin, DER 330) was procured from Dow Chemical Company. Diethylenetriamine (DETA), and 3-aminopropyltriethoxysilane (APTES) were purchased from Sigma-Aldrich. Stainless steel (SS), aluminum, polypropylene (PP), and polydimethylsiloxane (PDMS) sheets were purchased from the local market. *Staphylococcus aureus* (ATCC 6538), *Escherichia coli* (ATCC 25922), and phosphate-buffered saline (PBS) were obtained from Guangdong Institute of Microbiology. Mueller-Hinton broth (MHB) and Mueller-Hinton agar (MHA) were procured from Sigma-Aldrich. The LIVE/DEAD BacLight bacterial viability kit was purchased from Invitrogen (Carlsbad, CA).

Preparation of functionalized microsphere polystyrene (MPS). The preparation route of functionalized polystyrene microspheres (MPS) with antibacterial activity, metal ion chelating effect, and bacterially anti-adhesion is illustrated in Fig. 1. In the first step (step a), hydroxylated PS microspheres (HPS) were synthesized by dispersion polymerization of St and HEMA monomers using PVP as a stabilizer and AIBN as an initiator. Typically, 40 g of mixed solvents composed of ethanol and deionized water (mass ratio equals 9:1) were charged into a 100 mL round-bottom flask in a water-bath reactor which was equipped with a magnetic stirrer, thermometer, and reflux condenser, and 1.2 g PVP was then introduced into the above flask, a mixture containing 20 g St, 1.2 g HEMA, and 0.1 g AIBN was added dropwise into the flask in 2 h at 70 °C, the reaction was then kept for another 8 h. Finally, the obtained mixture was further cooled, the solvents were then removed by centrifugation, the centrifugal precipitants were further washed thrice by ethanol, the HPS microspheres were obtained after being dried at room temperature. MPS were further prepared by modifying the HPS microspheres with surface-grafted multifunctional copolymer P(VTES/GMA-IDA/BA/QAS/PEGMA). GMA-IDA monomer was firstly synthesized according to the reported literature.² Briefly, 13.37 g GMA was charged into the same above synthesis devices, and 7.52 g NaOH and 12.52 g IDA were dissolved in 60 g water, the obtained mixture was added dropwise into the flask for 1 h at 65 °C, the reaction was then kept for another 2 h, the final GMA-IDA was obtained. Thereafter, the copolymer P(VTES/GMA-IDA/BA/QAS/PEGMA) was synthesized as follows: 27 g ethanol was charged into the same above synthesis devices. The requisite amounts of GMA-IDA, QAS, BA, VTES, PEGMA and AIBN were added into 13 g ethanol, the mixture was then added dropwise into the flask for 2 h, the reaction was performed at 76 °C for 5 h to finally obtain the copolymer. Three different copolymers (P1, P2, and P3) were obtained by adjusting the contents of PEGMA monomers (10 wt%, 30 wt%, and 60 wt%), and the dosage of reactive monomers was illustrated in detail in Table 1. Ultimately, MPS were fabricated by grafting the copolymers as illustrated in step b of Figure 1. Firstly, 0.1 g PVP was dispersed into 95 % ethanol solution (17.9 g), in which the as-prepared MPS (2 g) was added under 30-min ultrasonication to obtain 10 wt% MPS dispersion. Afterwards, 10 wt% MPS dispersion (20 g) was mixed with 1.25 g copolymer solution, the pH was adjusted to 3 with hydrochloric acid, the hydrolysis and condensation reactions were then performed at 60 °C for 8 h. The final microspheres (MPS-1, MPS-2, and MPS-3) grafted with P1, P2, and P3 respectively were obtained after centrifugation and ethanol washing for three cycles.

Preparation of antibacterial micro/nano-structured MPS/Ag spheres. Micro/nano-structured MPS/Ag spheres were prepared by simply reducing [Ag(NH₃)₂]⁺ by PVP as illustrated in step c of Fig. 1. Typically, 0.08 g PVP was dissolved in 19 g ethanol, in which 0.15 g MPS microspheres were dispersed. Afterwards, 1 mL freshly prepared [Ag(NH₃)₂]⁺ aqueous solution with different concentrations (0.1, 0.3, 0.6 and 0.9 mol L⁻¹) was quickly added into the above MPS dispersion. The mixture was stirred at 70 °C for 6 h, further centrifuged, washed by ultrapure water, and dried at 60 °C in vacuum. The obtained microspheres were named MPS-2/Ag_{0.1}, MPS-2/Ag_{0.3}, MPS-

2/Ag_{0.6}, and MPS-2/Ag_{0.9}, respectively based on the MPS-2. The MPS-1/Ag_{0.9}, MPS-2/Ag_{0.9}, and MPS-3/Ag_{0.9} spheres were also prepared based on the MPS-1, MPS-2, and MPS-3, respectively.

Preparation of hydrophilic-type antibacterial and bacterially anti-adhesive surface. Hydrophilic-type antibacterial and bacterially anti-adhesive surface on 2 × 2 cm² stainless steel substrate was constructed as shown in step d of Fig. 1. The substrates were alternately washed with acetone, ultrapure water and ethanol thrice. Afterwards, 5 mg APTES (5 wt% ethanol solution) was sprayed on the substrate and then dried at 80 °C for 2 h. 0.1 g of MPS-1/Ag_{0.9}, MPS-2/Ag_{0.9}, or MPS-3/Ag_{0.9} microspheres were mixed with 10 mg DER 330 and 1 mg DETA solution in 0.05 mL benzyl alcohol and 1 mL ethanol, and the obtained mixture was further sprayed on the substrate. The amount of sprayed composite microspheres was about 1.2 mg cm⁻², afterwards, the coating on the substrate was further cured at 80 °C for 2 h. H-1, H-2, and H-3 were finally obtained based on the MPS-1/Ag_{0.9}, MPS-2/Ag_{0.9}, and MPS-3/Ag_{0.9}, respectively.

Preparation of hydrophobic-type antibacterial and bacterially anti-adhesive surface. The hydrophobic-type anti-adhesive surface was prepared by fabricating the as-prepared hydrophilic-type one with PFDTMS as illustrated in step e of Fig. 1. PFDTMS with predetermined amount (0.0025, 0.0125, 0.0625, and 0.5 mg·cm⁻²) in ethanol were prepared separately and adjusted pH to 10 with ammonia water, afterwards, the solution was sprayed-coating directly on H-2 surface and further dried at 80 °C for 3 h, the converted hydrophobic surfaces were named as F-1, F-2, F-3, and F-4, respectively.

Characterization and measurement. Chemical structure of multifunctional copolymer was characterized by FT-IR, recorded in KBr discs on a Bruker Vector 33 FT-IR spectrometer (Bruker Instruments Co., Germany). The surface morphologies of HPS, MPS and MPS/Ag were intuitively observed by a field-emission scanning electron microscopy (FESEM) (Merlin system, ZEISS) connecting with energy-dispersive X-ray spectroscopy (EDX, Model Inca400, Oxford Instruments). The surface elements of MPS/Ag were detected by X-ray photoelectron spectroscopy (XPS, Shimadzu-Kratos, Axis Ultra DLD, Japan). The content of silver loaded on the MPS microspheres was measured by ICP-AES (X Series 2, Thermo Fisher Scientific, American). Surface morphology and roughness were investigated by atomic force microscopy (AFM, Bruker Instruments Co., Germany). The swelling rate of various composite surfaces was carried out by microelectronic balance (Mettler Toledo Instruments Co., America) The water/oil contact angles (CA/OCA) and underwater OCA (UWOCA) of various droplets on different substrates or in the liquid were measured with a contact angle meter (OCA40 Micro, Dataphysics, Germany). The total surface free energies (γ_s) of hydrophobic-type antibacterial and bacterially anti-adhesive surface were calculated by combining the Owens-Wendt-Rabel-Kaelble (OWRK) and the Young eqs 1 and 2:

$$\gamma_s = \gamma_s^d + \gamma_s^p \quad (1)$$

$$(1 + \cos \theta)\gamma_L = 2(\gamma_s^d \gamma_L^d)^{1/2} + 2(\gamma_s^p \gamma_L^p)^{1/2} \quad (2)$$

where γ_s^d and γ_s^p are the dispersion and polar component of material surface, γ_L^d and γ_L^p are the dispersion and polar component of testing liquid,³ respectively. In this work, the testing surfaces were wetted by the specific liquids (deionized water and diiodomethane) with each predefined polar and dispersive component ($\gamma^p = 51.0$ mN m⁻¹, $\gamma^d = 21.8$ mN m⁻¹ for deionized water, and $\gamma^p = 2.3$ mN m⁻¹, $\gamma^d = 48.5$ mN m⁻¹ for diiodomethane, respectively).

Antibacterial activity assessment. Typical gram-negative and gram-positive bacteria including *S. aureus* (ATCC 6538) and *E. coli* (ATCC 25922) were employed for the antibacterial activity assessment. For the test, the bacterial suspensions containing 10⁷ colony forming units (CFUs) of bacteria were utilized, a sterile conical flask was charged with 38 mL PBS solution and 2 mL bacterial suspension, 0.8 mg of the antibacterial microsphere samples were charged into the conical flask and then incubated with a shaking incubator at 37 °C with a speed of 150 rpm for 6 h. Afterwards, 100 μ L bacteria suspension after antibacterial testing was taken out and serially diluted with a dilution factor of ten, 20 μ L of diluted bacterial suspension was taken and dropped into the MHA plates in the Petri dishes, and then incubated at 37 °C for 24 h. The number of bacteria was calculated by multiplying the counted number of colonies and the dilution factor. Untreated stainless steel was also tested as the control, the antibacterial rate was calculated as eq (3).

$$\text{Antibacterial rate (\%)} = \frac{A - B}{A} \times 100\% \quad (3)$$

where A represents the average number of bacteria on the control (CFU_{control} mL⁻¹) and B represents the average number of bacteria on the test samples (CFU_{sample} mL⁻¹).

MIC and MBC determination of antibacterial microspheres. The MHB was employed as the bacterial nutrient growth medium for the evaluation of minimum inhibitory concentration (MIC) and was freshly prepared (within 1 week). Serial 2-fold dilutions of antibacterial monomers were prepared in a series of tubes, with gradient concentration ranging from 0.02 to 0.08 mg mL⁻¹. Each sterile test tube was then charged with 4 mL of MHB, 2 mL of bacteria suspension at 10⁶ CFU mL⁻¹, and 2 mL of the above antibacterial microspheres dilution, which were adjusted to final concentrations with 0.02, 0.04, and 0.08 mg mL⁻¹, respectively. The testing tubes were further incubated with a shaking incubator at 37 °C with a speed of 150 rpm for 6 h. The minimum concentration was taken as the MIC of antibacterial microspheres at which there was no visible turbidity. The MIC measurement was done in triplicate to confirm the value of MIC for each type of bacteria. For determination of minimum bactericidal concentration (MBC), MHA was employed as the bacterial growth medium. The MHA was poured onto sterilized Petri dishes to be solidified to form MHA plate. 100 μL of bacterial culture was taken out from the test tubes in the MIC test, further inoculated uniformly onto the surface of MHA plate, and then incubated at 37 °C for 24 h. All the experiments were performed in triplicate, the results were mean values.

Durably antibacterial microspheres testing. Nanosilvers on microspheres would be completely released due to its release-killing property. Durably antibacterial properties of the antibacterial MPS/Ag microspheres after completely releasing the loaded nanosilvers was investigated by cyclic antibacterial test, after dissolving nanosilvers by the hydrochloric acid for 6 h, the treated microspheres powder preserving QAS of contact-killing property was obtained after be dried, and antibacterial experiments was repeatedly performed for the same sample, the antibacterial rate was measured after each cycle.

Bacterial anti-adhesion of the treated surface. Bacterial anti-adhesion of the hydrophilic/hydrophobic-type surfaces were evaluated by the method as reported by Oh *et al.*⁴ and Cao *et al.*⁵ with a little alteration. The samples (hydrophilic-type H-1, H-2, and H-3, hydrophobic-type F-1, F-2, F-3, and F-4, and the pristine SS as control) with 1 × 1 cm were vertically immersed into 10 mL of bacterial suspension (*S. aureus* or *E. coli*) with 10⁷ CFU mL⁻¹, and incubated under static conditions for 4 h at 37 °C. Then the testing samples were drawn along vertical direction from the bacterial suspension and held vertically for 2 min to allow unadhered bacteria to slide away, and transferred into a tube with 25 mL of fresh MHB, and further incubated for 24 h at 37 °C at a shaking speed of 120 rpm. Afterwards, the samples were taken out using sterile forceps and washed triple with 5 mL of sterile water to wash away the unadhered bacteria. Then the samples were put into another tube containing 5 mL of PBS solution, those strongly adhered were then detached from the surface by ultrasonication for 2 minutes. The same operation was performed for five times. The above detached bacteria in PBS solution were then homogenized by a Tissue Tearor homogenizer, and then 100 μL of this solution spread onto the MHA plates, and further incubated at 37 °C for 24 h. The actual number of adhered bacteria was calculated by multiplying the counted number of colonies and the dilution factor. Bacterial anti-adhesion rate is estimated as eq (4):

$$\text{Bacterial anti-adhesion rate (\%)} = (\text{CFU}_{\text{control}}\text{mL}^{-1} - \text{CFU}_{\text{sample}}\text{mL}^{-1}) / \text{CFU}_{\text{control}}\text{mL}^{-1} \quad (4)$$

where CFU_{control} mL⁻¹ represents the number of the viable bacteria per unit volume culture for the pristine sample, CFU_{sample} mL⁻¹ represents the number of the viable bacteria per unit volume culture for the treated composite sample.

Morphology of bacterial adhesion on the surface. The bacterial attachment by *S. aureus* and *E. coli* on the treated surface was observed by SEM after performing the bacterial anti-adhesive experiments. Samples were treated before testing as follows. Firstly, the samples were washed thrice with sterile PBS, then fixed with 4 wt% glutaraldehyde solution for 2 h, and washed twice with phosphate buffer and once again with distilled water. Then the fixed bacteria were dehydrated with a series of gradient ethanol solution (50, 75, 90, and 100 wt%) for fifteen minutes. Afterwards, all

the samples were dried completely in a ventilation, then pre-coated with platinum at 30 mA for 2 min and further observed by FESEM.

Live/Dead bacterial viability assay. Live/dead bacterial viability assays were utilized to intuitively assess antibacterial activities of samples (HPS, MPS-2/Ag_{0.1}, MPS-2/Ag_{0.3}, MPS-2/Ag_{0.6}, MPS-2/Ag_{0.9}, and the control). After antibacterial activity experiment, 100 μ L bacteria suspension was taken out, placed in a test tube, and were further stained by injecting 25 μ L fluorescent dye mixture of a green SYTO9 and red propidium iodide (PI) for 15 min. 100 μ L stained bacteria suspension was transferred onto the slide glass, and covered with a piece of glass cover slip. The thorough staining of bacteria was performed to carry out at room temperature in darkness for 15 min. Thereafter, the bacteria were intuitively observed under an Olympus BX51 epifluorescence microscope using green and red filters with excitation/emission 440-480/515- 540 nm and 540-560/630-660 nm, respectively.

MD simulation methods: To investigate the resistance of the lipophilic substance on the hydrophilic surface of PEGMA so as to study the bacterially anti-adhesive property, molecular dynamics (MD) simulation was conducted to estimate the dynamic behavior of benzene molecules on the surface of PEGMA with and without H₂O. PEGMA, benzene and H₂O were described by the Lennard-Jones (LJ) and electrostatic potentials. The LJ potential parameters were adopted from the universal force field,⁶ and the atomic charges of PEGMA, benzene and H₂O molecules were estimated using the Qeq method.⁷ Firstly, thirty PEGMA simple chains were established using Amorphous Cell module in Materials Studio. To calculate the dynamic behavior of benzene, all structures were first optimized by the Forcite module in Materials Studio, and then MD simulation toward the benzene-PEGMA systems with or without H₂O was performed at 298 K for 15 ns using the same module. With the addition of H₂O molecules, the interaction energies between the benzene and PEGMA molecules were estimated for the final structures after MD simulation. All of LJ interactions were evaluated with a cutoff of 12 Å, and the electrostatic interactions were estimated using the Ewald summation method with an accuracy of 10⁻³ kcal mol⁻¹.

Swelling ratio assessment: the swelling ratio of the different samples was assessed by immersing the samples in deionized water for 24 h. The swelling ratio was taken as the ratio of the difference between the wet weight and the dried weight to the dried weight of the samples. For each condition, three independent tests were conducted and the average value obtained taken as the final swelling ratio of the sample, the swell rate was calculated as eq (5).^{11, 12}

$$\text{Swelling ratio (\%)} = \left(1 - \frac{W_{dry}}{W_{wet}}\right) \times 100\% \quad (5)$$

Where W_{wet} is the weight of the wet samples, W_{dry} is the weight of the dry samples.

Antibacterial and bacterially anti-adhesive durability of treated surface. The mechanical abrasion resistance of the as-prepared antibacterial and bacterially anti-adhesive surfaces was assessed by an abrasion-resistance machine (Model-339, Dongguan City Dazhong Instrument Co., Ltd.), on which a reciprocating shaft with 200 g loading (corresponding to a standard normal stress of ca. 27 kPa) was pressed onto the test surface, a moving cycle from back to forth was calculated as one-time abrasion. The mechanical damages of the films after 30-times wearing were investigated by SEM. Impact resistance of antibacterial and bacterially anti-adhesive surface was measured by a DuPont impact tester, the test specimen was impacted by a 1 kg falling impact head to drop freely onto the surface from a certain height, its consequent damage or deformation was then checked. The chemical stability of the as-prepared antibacterial and bacterially anti-adhesive surface was performed by immersing the specimens into the hydrochloric acid (pH=1), sodium hydroxide (pH=14), and sodium chloride solutions (1mol L⁻¹) for 16 h. Ultimately, the antibacterial and bacterially anti-adhesive rate were investigated after the mechanical and chemical resistance test. Additionally, a longer culture time of bacteria was conducted to further confirm the durably bacterial anti-adhesion performance of hydrophobic-type surface, the typical F-4 surface was selected and culture time was 24 h, all of procedures were exactly the same to above the bacterial anti-adhesion assessment method. All the experiments were performed in triplicate, and the results were mean values.

Table 1. Percentage of the monomers for the as-prepared copolymers.

Samples	GMA-IDA	QAS	PEGMA	BA	VTES
	(wt%)	(wt%)	(wt%)	(wt%)	(wt%)
P1	20	2	10	58	10
P2	20	2	30	38	10
P3	20	2	60	8	10

Table S2. Contact angle of diverse bacterial suspension droplets on different substrates.

Bacterial suspension	Substrates							
	PDMS		PP		Aluminum		SS	
	Untreated	Treated	Untreated	Treated	Untreated	Treated	Untreated	Treated
Water	99.8	158.3	98.8	155.3	78.7	152.9	70.8	154.1
Coffee	96.5	152.3	93.3	152.9	71.5	152.5	61.7	153.3
Milk	93.1	152.9	83.7	150.1	62.7	150.4	58.4	150.9
Coco coca	94.5	154.3	95.1	153.7	79.1	152.1	59.3	152.3
Tea	97.7	154.1	94.4	153.3	75.3	150.9	60.4	151.4
Blood	91.9	152.8	80.3	154.9	67.7	150.7	49.2	152.2

Supplementary discussion

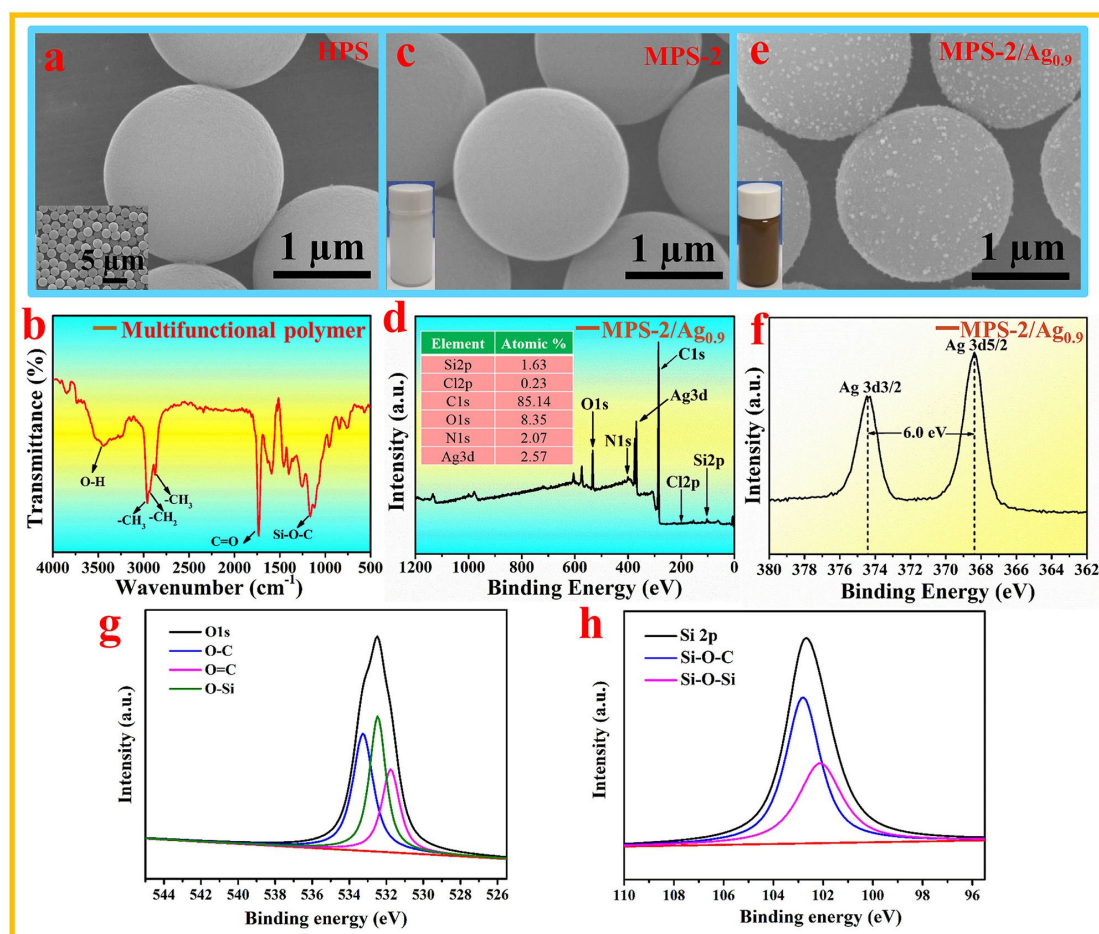


Figure S1. SEM images of (a) HPS, (c) MPS-2, (e) MPS-2/Ag_{0.9}. FT-IR spectra of the multifunctional polymer (b). XPS survey spectrum (d) and high-resolution XPS spectrum (f) of Ag 3d for MPS/Ag_{0.9}, the corresponding deconvoluted O 1s (g) and Si 2p (h) peaks of composite microspheres.

Supplementary explanation

As depicted in Figure S1a, hydroxylated HPS microspheres with diameters of around 2 μm were successfully prepared and uniformly distributed. Afterward, by grafting with P-2, the obtained MPS-2 microspheres were endowed with antibacterial activity, a metal ion chelating effect, and bacterial anti-adhesion. The chemical structure of the grafted polymer P-2 was analyzed by Fourier-transform infrared spectroscopy (FT-IR), as shown in Figure S1b. The polymer was mainly characterized by the bands at 3421 cm^{-1} (ν O-H and ν N-H), 2959 cm^{-1} (ν_{as} C-H of -CH₃), 2933 cm^{-1} (ν_{as} C-H of -CH₂), 2874 cm^{-1} (ν_{as} C-H of -CH₃), 1732 cm^{-1} (ν C=O), and the generated peaks at 1165 cm^{-1} (ν_{s} Si-O-C). After being decorated with Ag, the MPS-2/Ag suspension turned from the white MPS-2 to yellow (insets of Figure S1c and S1e). As expected, the Ag nanoparticles were uniformly distributed on the surface of MPS-2/Ag (Figure S1e) with a uniform size \sim 40 nm because a large number of carboxyl groups in the GMA-IDA molecular chain grafted on the MPS microspheres adsorbed the Ag⁺ in the silver ammonia solution, which was further reduced to nanosilver under the reduction of PVP and loaded onto the surface of the microspheres.⁸ As illustrated in a wide survey of XPS spectra (Figure S1d), the characteristic signals of O 1s (\sim 532.56 eV), N 1s (\sim 400.04 eV), C 1s (\sim 284.8 eV),

Cl 2p (~197.37 eV), and Si 2p (~102.63 eV) were clearly observed, with their element atomic ratios summarized in the inset table of Figure S1d. From Figure S1f, Ag 3d_{5/2} and Ag 3d_{3/2} were further confirmed by the high-resolution XPS spectra with peaks at 368.4 and 374.4 eV, respectively. The loaded Ag nanoparticles on the surface of the composite microspheres were indicated by a difference of 6.0 eV between the Ag 3d_{5/2} and Ag 3d_{3/2} peaks.^{9,10} Furthermore, the corresponding deconvoluted O 1s peaks of O-C (~533.2eV), O=C (~531.7eV), and O-Si (~532.4 eV) (Figure S1 g), and the deconvoluted Si 2p peaks of Si-O-C (~102.8 eV), and Si-O-Si (~102.1 eV) (Figure S1 h) confirmed the successful grafting of HPS microspheres by the multifunctional polymer and well-preparation of the MPS-2/Ag_{0.9} composite microspheres, the results were good agreement with the previously reported literatures.¹³⁻¹⁷

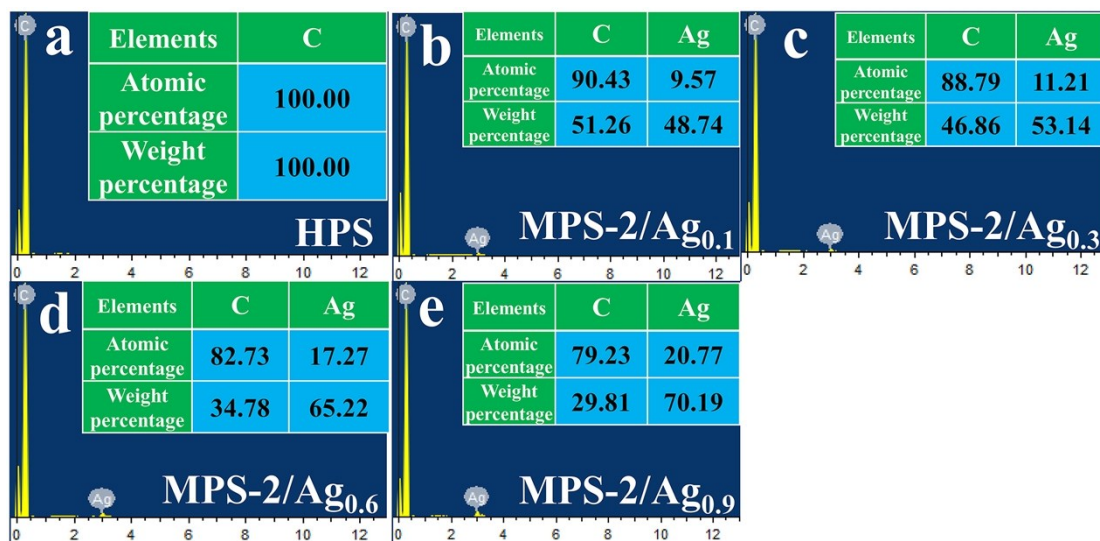


Figure S2. EDX results of HPS (a), MPS-2/Ag_{0.1} (b), MPS-2/Ag_{0.3} (c), MPS-2/Ag_{0.6} (d), MPS-2/Ag_{0.9} (e).

Supplementary explanation

The atomic percentage of silver on their surfaces gradually increased from HPS to MPS-2/Ag_{0.9} (0, 9.57 %, 11.21 %, 17.27 %, and 20.77% for HPS, MPS-2/Ag_{0.1}, MPS-2/Ag_{0.3}, MPS-2/Ag_{0.6}, and MPS-2/Ag_{0.9}, respectively).

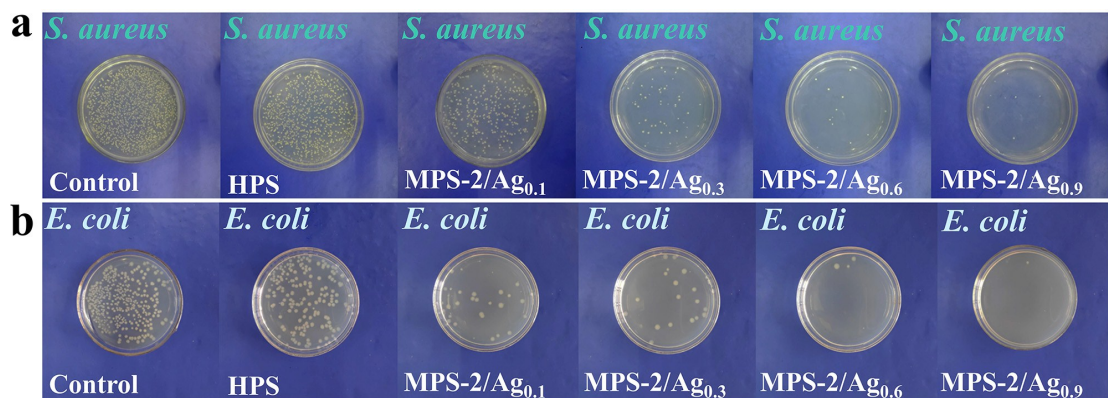


Figure S3. Bacterial colonies formation of *S. aureus* (a) and *E. coli* (b) with different loaded silver of MPS-2/Ag composite microspheres.

Supplementary explanation

The antibacterial rate both for *S. aureus* and *E. coli* significantly increased with increasing amount of loaded silver (MPS-2/Ag_{0.1}, MPS-2/Ag_{0.3}, MPS-2/Ag_{0.6}, and MPS-2/Ag_{0.9} against *S. aureus*: 76 %, 96.3 %, 98.7 %, and 99.5 %, respectively, and against *E. coli*: 92.4 %, 97.1 %, 99.4 %, and 99.9 %, respectively), as compared with 11.5 % and 20.3 % for HPS against *S. aureus* and *E. coli*, respectively, indicating that the MPS-2/Ag exhibited excellent antibacterial property which could be adjusted by loading different amount of silver.

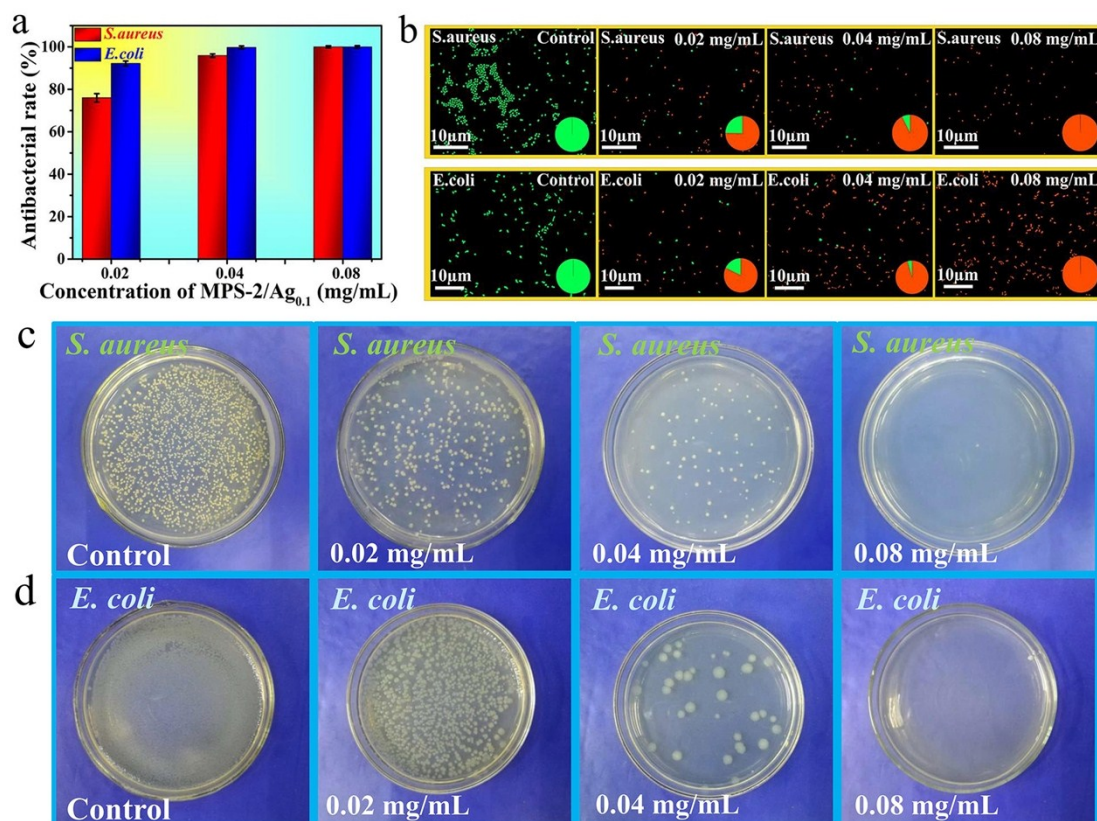


Figure S4. (a) Antibacterial rate of MPS-2/Ag_{0.1} composite microspheres in the bacterial suspension with different concentrations of 0.02, 0.04, and 0.08 mg mL⁻¹. (b) Fluorescence microscope images of the control and MPS-2/Ag_{0.1} with different concentrations in the bacterial suspension of 0.02, 0.04, and 0.08 mg mL⁻¹. Bacterial colonies formation of *S. aureus* (c) and *E. coli* (d) with different concentration of MPS-2/Ag_{0.1} composite microspheres.

Supplementary explanation

Inhibitory and bactericidal properties of MPS/Ag composite microspheres against bacteria. MPS-2/Ag_{0.1} with the lowest content of silver was chosen to investigate the minimum inhibitory concentration (MIC) for the assessment of the inhibitory ability with the lowest concentration, as shown in Figure S4a, and the plate count experiment in Figure S4c, d. The antibacterial rate of MPS-2/Ag_{0.1} for both *S. aureus* and *E. coli* significantly improved with increasing the concentration of composite microspheres, and finally reached above 99.99 % against both *S. aureus* and *E. coli*. Almost no bacteria survived, when 0.08 mg mL⁻¹ was considered as the MIC value. Afterwards, the MBC value was observed to further illustrate the bactericidal ability of MPS-2/Ag as shown in Figure S4c, d, the MBC value was 0.08 mg mL⁻¹. After MBC test, the bacteria were further stained with fluorescence, the results of live/dead bacterial viability in Figure S4b demonstrated that the densities of live bacteria were drastically declined, conversely, the densities of dead bacteria were greatly increased. On the basis of the aforementioned results, the prepared MPS-2/Ag showed excellent inhibitory and bactericidal properties.

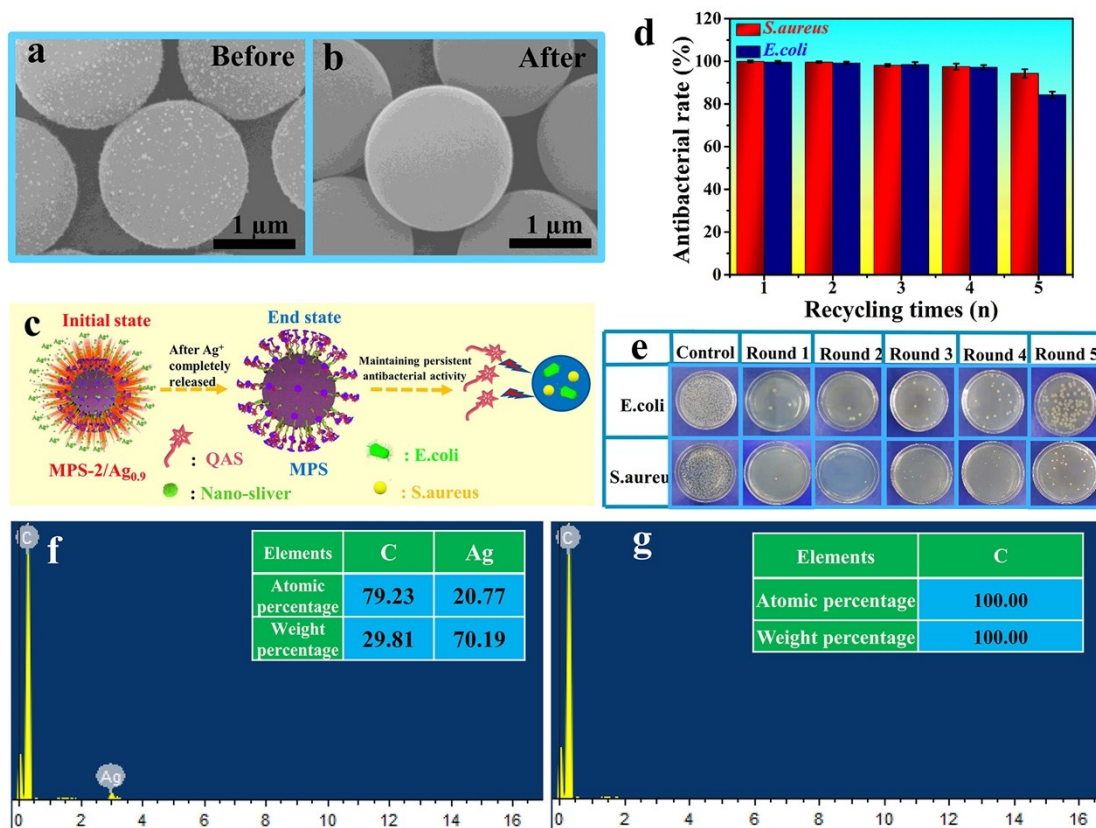


Figure S5. (a-b) SEM images of MPS-2/Ag_{0.9} before and after releasing nanosilvers. (c) Schematic diagram for the model of releasing nanosilvers. (d) Antibacterial rate of MPS-2/Ag_{0.9} after completely releasing nanosilvers for different recycling times. (e) Photographs of the agar plates of *S. aureus* and *E. coli* treated with different recycling times. (f) and (g) the EDX results of MPS-2/Ag_{0.9} before and after silver ions releasing completely.

Supplementary explanation

Antibacterial durability of MPS-2/Ag composite microspheres. Despite the fact that silver-based antibacterial materials exhibit a high biocidal efficacy due to their high efficiency of Ag⁺ releasing, a real problem is that high biocidal efficacy may be gradually weakened after being used for some time. Herein, incorporating the non-dissolution-type QAS groups into the MPS-2/Ag was aimed to maintain the antibacterial durability while the silver ions were completely released. As shown in Figure S5b, silver nanoparticles on the MPS-2/Ag_{0.9} disappeared after acid treatment for 6 h, as compared to that before treatment (Figure S5a), indicating that the silver ions were released completely. Additionally, EDX results (Figure S5f, g) implied the silver element atomic percentage changed from 20.77 % to 0 %, which is well-consistent with SEM images. As schematic diagram for releasing nano-silver depicted in Figure S5c, the newly generated MPS-2 after Ag⁺ released completely (in the end state) from MPS-2/Ag_{0.9} (in the initial state) retained a large number of QAS groups, and maintained persistent antibacterial activity. From Figure S5d and Figure S5e, the antibacterial rate only slowly decreased to 96.3 % and 84.3 %, respectively, against *E. coli* and *S. aureus* after five cycles in the absence of silver nanoparticles. Therefore, the combination of silver nanoparticles and QAS incorporated polymers resulted in a synergistic antibacterial effect together with excellent antibacterial durability.

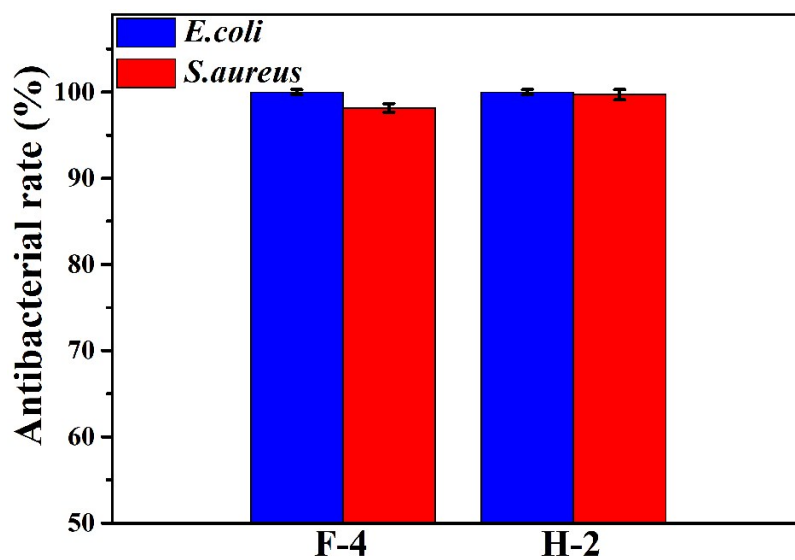


Figure S6. Antibacterial rate of hydrophobic-type F-4 and hydrophilic-type H-2 surfaces.

Supplementary explanation

The obtained hydrophilic-type antibacterial H-2 surface exhibited outstanding antibacterial rate of 99.99 % and 99.99 % against *E. coli* and *S. aureus*, respectively. After fluorination, a slight decrease of antibacterial rate (99.7 % and 98.15 % against *E. coli* and *S. aureus*, respectively) of F-4 demonstrated the fluorination modification had almost no effect on the antimicrobial activity.

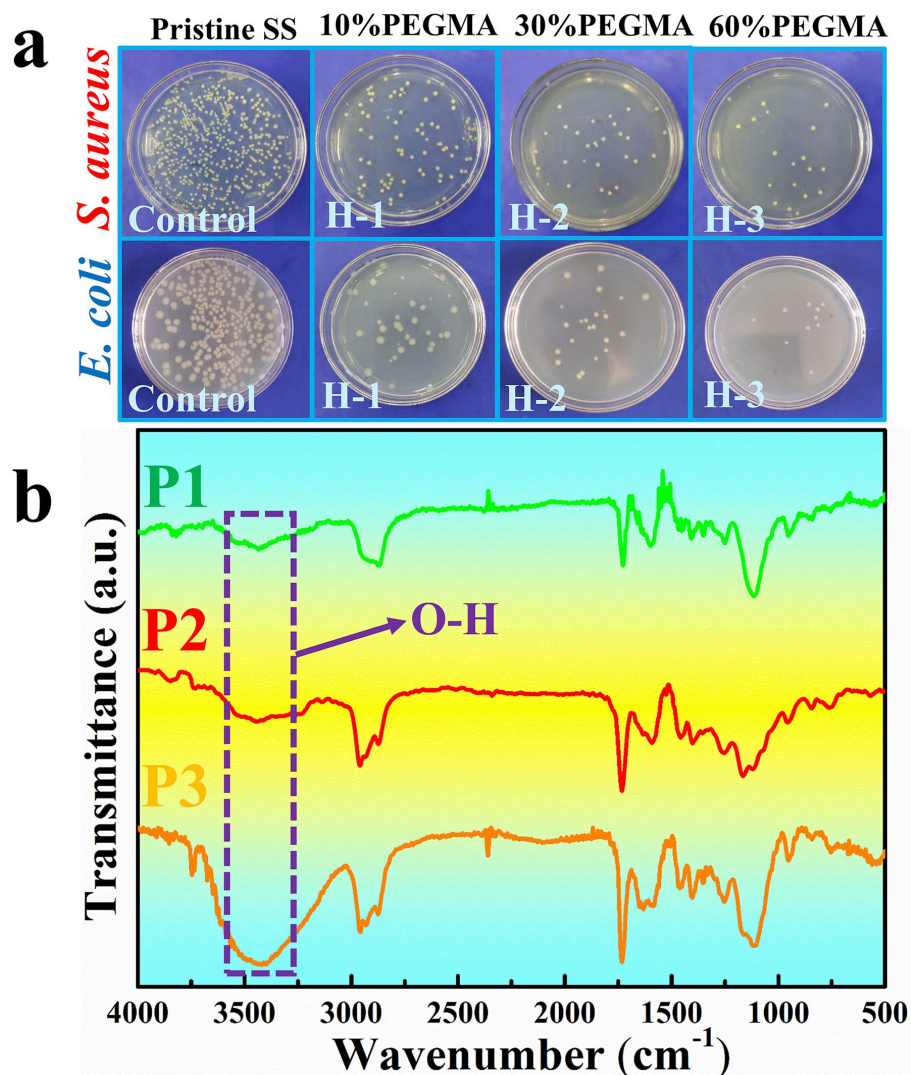


Figure S7. (a) Bacterial colonies formation of *S. aureus* and *E. coli* treated with H-1, H-2, H-3 of hydrophilic-type surfaces. (b) FT-IR image of different weight concentration PEGMA in multifunctional polymer.

Supplementary explanation

The results of bacterial anti-adhesion testing demonstrated that bacterial anti-adhesion rate of MPS/Ag_{0.9} treated on stainless steel substrate gradually increased (*S. aureus*: 77.3 %, 92.7 %, and 94.9 % for H-1, H-2, and H-3, respectively. *E. coli*: 84.7 %, 93.3 %, and 96.3 % for H-1, H-2, and H-3, respectively) with increasing introduced hydrophilic PEGMA component. Their stretching vibration peak of hydroxyl group at 3421 cm^{-1} gradually intensified with the increase of PEGMA.

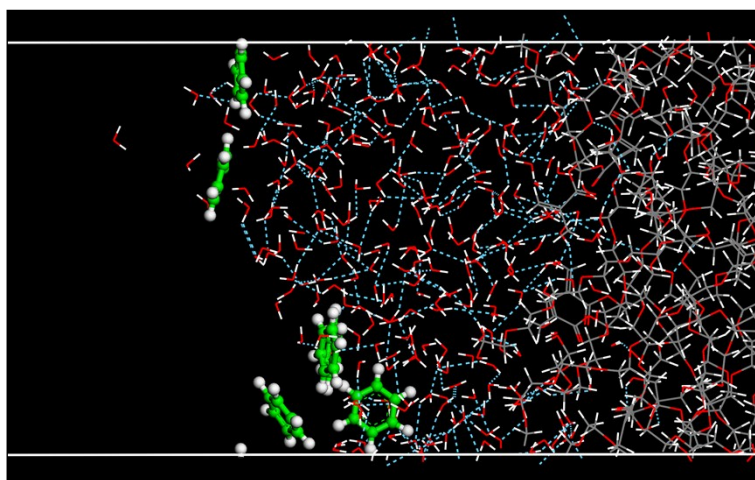


Figure S8. Hydrogen bonds between H₂O and polymer.

Supplementary explanation

The hydration layer mainly causes by frozen water. In our simulation, a water layer was added in the initial model. During MD simulation, these H₂O molecules could be allowed the free movement, and finally they form the structure of hydration layer, because of the strong and stable hydrogen bonds between H₂O and polymer, as shown in Figure S8. The formation of hydration layer using MD simulation is similar as Jiang Shaoyi *et al*'s works.^{16,17}

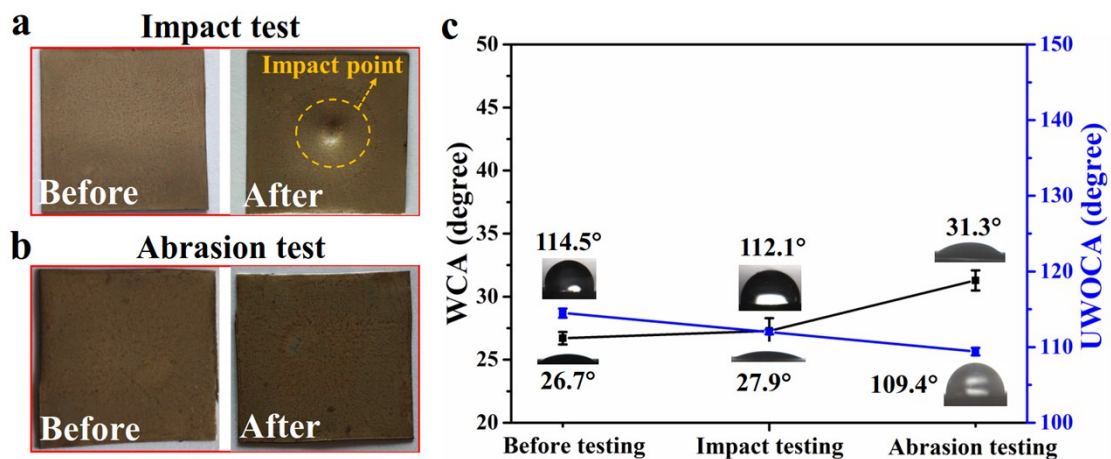


Figure S9. Real pictures of the hydrophilic H-2 surface before and after impact test (a), abrasion test (b), WCAs and UWOCAs of H-2 surface before and after the impact test and abrasion test (c).

Supplementary explanation

It was found that no film falling was observed after the impact and 30 cycles of abrasion tests. The hydration layer was not affected as demonstrated in a little change of the WCAs and UWOCAs (WCAs were 26.7°, 27.9°, and 31.3°, UWOCAs were 114.5°, 112.1°, and 109.4°, for the H-2 surface before test, after impact and abrasion tests, respectively). It was indicated that this hydrophilic-type bacterial anti-adhesive surface exhibited robust resistance to the mechanical damage.

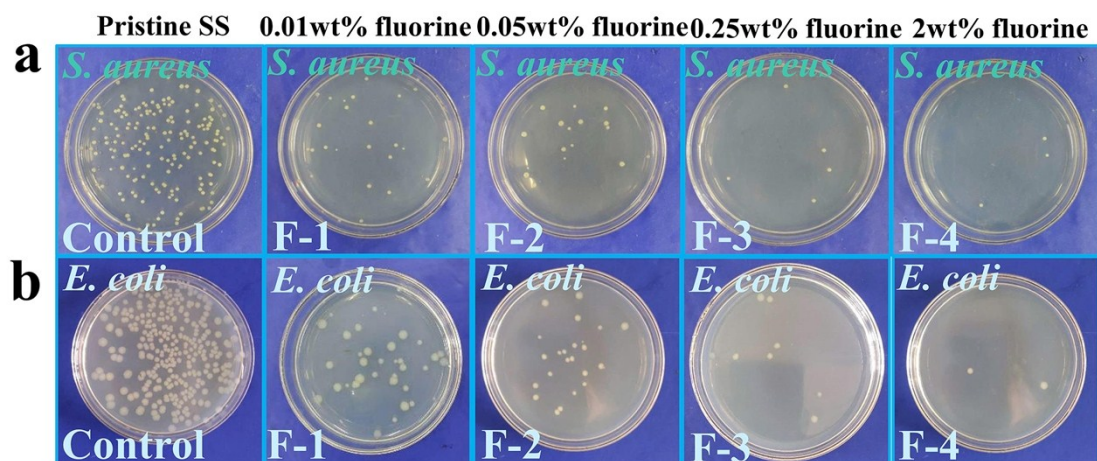


Figure S10. Bacterial colonies formation of *S. aureus* (a) and *E. coli* (b) treated with F-1, F-2, F-3, F-4 of hydrophobic-type surfaces.

Supplementary explanation

The results of bacterial anti-adhesion testing quantitatively demonstrated the bacterial anti-adhesion rate of the hydrophobic fluoroalkylsilane treated MPS-2/Ag composite surfaces gradually increased with the improvement of introducing fluorine component (*S. aureus*: 85 %, 91.1 %, 96.7 %, and 98.3 % for F-1, F-2, F-3, and F-4, respectively. *E. coli*: 88.1 %, 92.7 %, 97.3 %, and 99.4 % for F-1, F-2, F-3, and F-4, respectively).

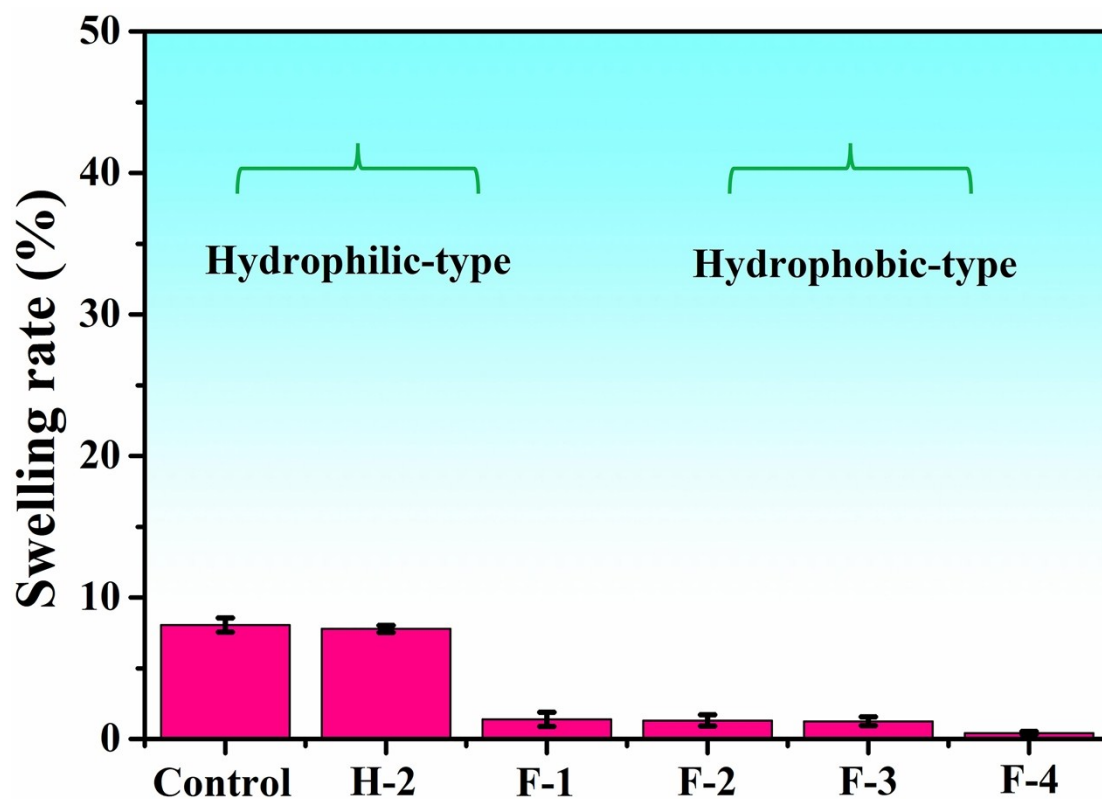


Figure S11. The swelling rate of different samples. (Control with no F and EP), H-2, F-1, F-2, F-3, and F-4, respectively.)

Supplementary explanation

The swelling rate with 8.05 % was indicated for the control with no F and EP, and no obvious decrease (7.78 %) for the H-2 after introducing the EP, indicating that EP would not restrict the swelling action of the PEGMA. However, after fluorination, obvious decrease was demonstrated with the swelling rate of 1.38 %, 1.31 %, 1.25 %, and 0.42 % for the F-1, F-2, F-3, F-4, respectively. It was indicated that the hydration layer was indeed influenced by the PFDTMS.

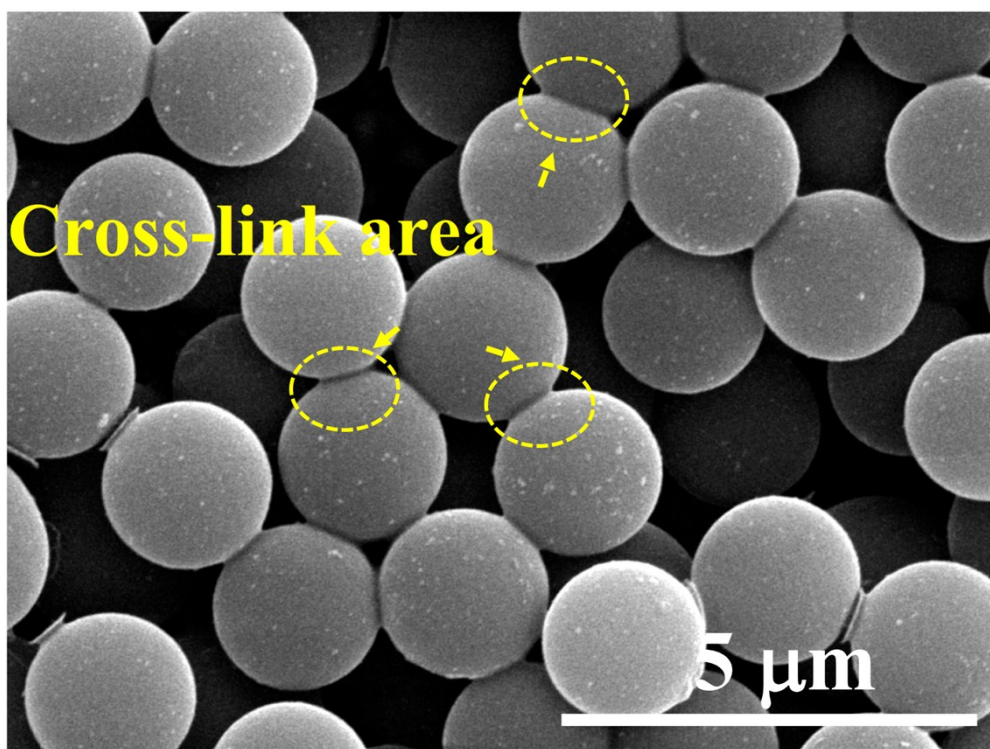


Figure S12. SEM image of the hydrophobic-type F-4 composite surface.

Supplementary explanation

It was observed that the AgNPs on the surface of MPS microspheres were not embedded in epoxy resin layer and fluorosilane, epoxy resin was gotten together at the junction among the microspheres after volatilization of the solvent.

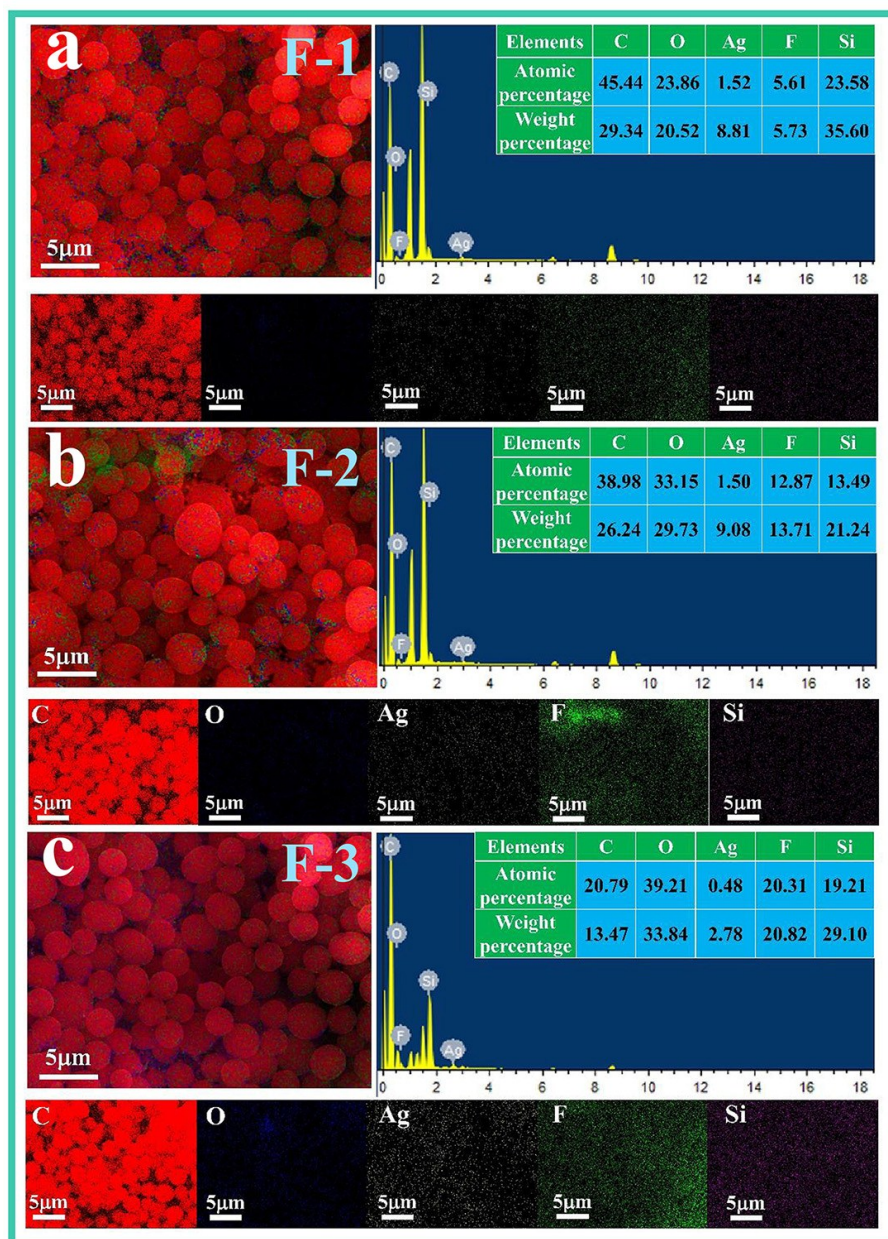


Figure S13. SEM-EDX mapping of treated with different percentage fluorine composition of hydrophobic-type surfaces (F-1 (a), F-2 (b), and F-3 (c)).

Supplementary explanation

The elements were uniformly distributed on the hydrophobic-type surfaces, the exact content of fluorine element for F-1, F-2, F-3 and F-4 is 5.6 wt%, 12.87 wt%, 20.31 wt%, and 46.81 wt%, respectively.

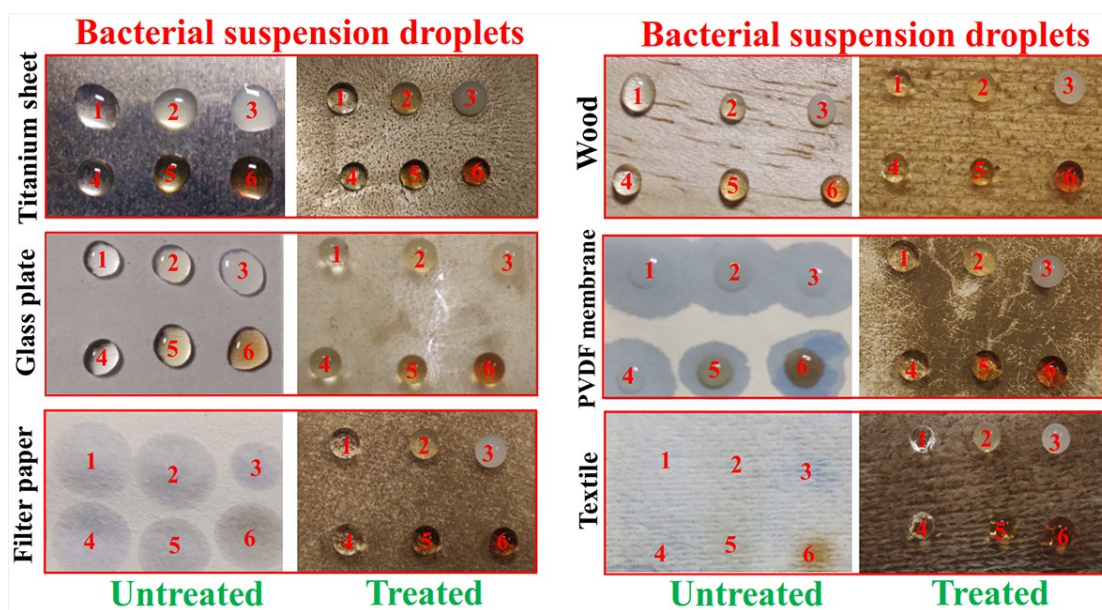


Figure S14. Images of 20 μL diverse 10^8 CFU mL^{-1} bacterial suspension droplets (in water (1), coffee (2), milk (3), cola (4), tea (5), and animal blood (6)) placed on the untreated and the treated substrates (titanium sheet, glass plate, filter paper, wood, PVDF membrane, and textile).

Supplementary explanation

It was obviously shown that various bacterial droplets spread on the untreated substrates with small static contact angles, especially for the PVDF membrane, filter paper, glass plate, and textile. Compared to the untreated surfaces, it was obviously observed that all the bacterial suspension droplets on the treated superhydrophobic-type composite surfaces exhibited excellent liquid-repellent capability, including titanium sheet, glass plate, filter paper, wood, PVDF membrane, and textile.

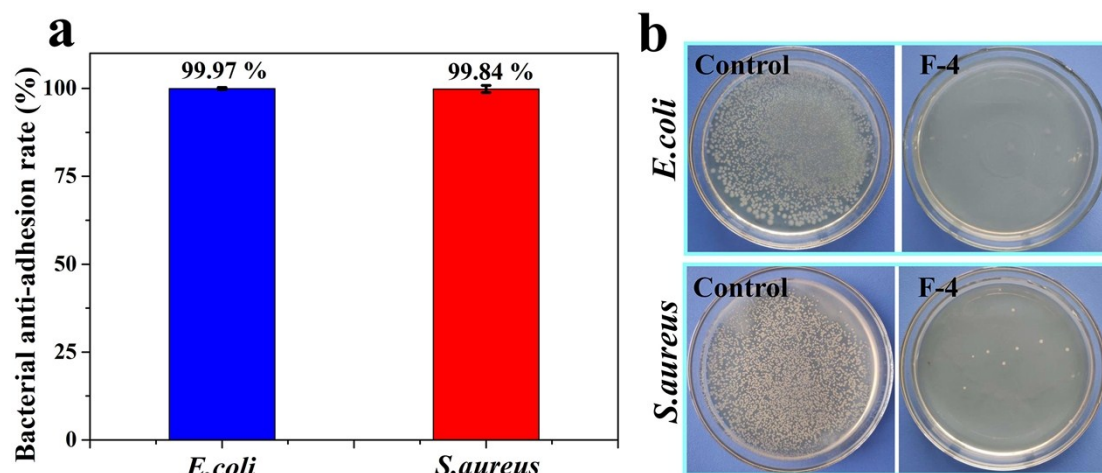


Figure S15. Bacterially anti-adhesive rate (a) and bacterial colonies formation of *S. aureus* and *E. coli* (b) treated with hydrophobic-type F-4 surfaces with the bacteria cultural time of 24 h.

Supplementary explanation

The bacterially anti-adhesive rate of F-4 surface for *E. coli* and *S. aureus* was 99.97 % and 99.84 %, respectively, which exhibited durably bacterial anti-adhesion properties.

References

- [1] J. Lin, X. Y. Chen, C. Y. Chen, J. T. Hu, C. L. Zhou, X. F. Cai, W. Wang, C. Zheng, P. P. Zhang, J. Cheng, Z. H. Guo and H. Liu, *ACS Appl. Mater. Interfaces*, 2018, **10**, 6124–6136.
- [2] X. X. Li, Q. Q. Wang, X. Y. Dong, Y. Liu and Y. Sun, *Biochem. Eng. J.*, 2018, **138**, 74–80.
- [3] S. G. Chen, S. J. Chen, S. Jiang, Y. M. Mo, J. X. Luo, J. N. Tang and Z. C. Ge, *Colloid Surface B*, 2011, **85**, 323–329.
- [4] J. K. Oh, X. X. Lu, Y. J. Min, L. Cisneros-Zevallos and M. Akbulut, *ACS Appl. Mater. Interfaces*, 2015, **7**, 19274–19281.
- [5] F. F. Cao, E. G. Ju, Y. Zhang, Z. Z. Wang, C. Q. Liu, Y. Y. Huang, K. Dong, J. S. Ren and X. G. Qu, *ACS Nano*, 2017, **11**, 4651–4659.
- [6] A. K. Rappe, C. J. Casewit, K. S. Colwell, W. A. Goddard, and W. M. Skiff, *J. Am. Chem. Soc.*, 1992, **114**, 10024–10035.
- [7] A. K. Rappe and W. A. Goddard, *J. Phys. Chem.*, 1991, **95**, 3358–3363.
- [8] K. Zhao, J. Zhao, C. J. Wu, S. W. Zhang, Z. W. Deng, X. X. Hu, M. L. Chen and B. Peng, *Rsc Adv.*, 2015, **5**, 69543–69554.
- [9] Y. Z. Zhang, X. M. Liu, Z. Y. Li, S. L. Zhu, X. B. Yuan, Z. D. Cui, X. J. Yang, P. K. Chu and S. L. Wu, *ACS Appl. Mater. Interfaces*, 2018, **10**, 1266–1277.
- [10] G. F. Liao, J. Chen, W. G. Zeng, C. H. Yu, C. F. Yi and Z. S. Xu, *J. Phys. Chem. C.*, 2016, **120**, 25935–25944.
- [11] Y. Shi, C. B. Ma, L. L. Peng and G. H. Yu, *Adv. Funct. Mater.*, 2015, **25**, 1219–1225.
- [12] A. Venault, Y. N. Chou, Y. H. Wang, C. H. Hsu, C. J. Chou, D. Bouyer, K. R. Lee and Y. Chang, *J. Membrane. Sci.*, 2018, **547**, 134–145.
- [13] A. Abdolmaleki, S. Mallakpour and M. Rostami, *Prog. Org. Coat.*, 2015, **80**, 71–76.
- [14] N. B. Pramanik and N. K. Singha, *Rsc Adv.*, 2015, **5**, 94321–94327.
- [15] D. H. Zhu, X. Y. Nai, S. J. Lan, S. J. Bian, X. Liu and W. Li, *Appl. Surf. Sci.*, 2016, **390**, 25–30.
- [16] R. Shao, J. Niu, F. Zhu, M. L. Dou, Z. P. Zhang and F. Wang, *Nano Energy*, 2019, **63**, 103824.

- [17] X. F. Zhang, L. X. Chen, J. Yun, X. D. Wang and J. Kong, *J. Mater. Chem. A*, 2017, **5**, 10986–10997.
- [18] J. Zheng, L. Y. Li, S. F. Chen and S. Y. Jiang, *Langmuir*, 2004, **20**, 8931–8938.
- [19] Y. He, J. Hower, S. F. Chen, M. T. Bernards, Y. Chang and S. Y. Jiang, *Langmuir*, 2008, **24**, 10358–10364.